

Seismic Behavior of Steel Buildings with Combined Rigid and Semi-Rigid Frames

Bülent AKBAŞ

*Department of Earthquake and Structural Science, Gebze Institute of Technology,
41400 Gebze, Kocaeli-TURKEY*

Jay SHEN

*Department of Civil and Architectural Engineering, Illinois Institute of Technology,
Illinois 60616-3793 USA*

Received 27.01.2003

Abstract

The 1994 Northridge Earthquake (USA) has shown the vulnerability of welded moment connections in steel moment resisting frames (MRFs) subject to severe earthquake ground motions (EQGMs). Since then, as an alternative connection type, bolted connections, often called semi-rigid connections, are considered for the retrofit and new design of steel MRFs in high seismicity regions. This paper investigates the seismic design and performance of a hybrid system, consisting of welded moment frames and bolted semi-rigid frames. For this purpose, an analytical study is carried out on two steel buildings with interior semi-rigid steel frames having beam-to-column connections with different strength and stiffness ratios. The two buildings, of 5 and 10 stories, are designed in compliance with the current seismic design codes for two different cases. In the first case (Case 1), the interior frames are assumed to be simply connected. In the second case (Case 2), the interior frames are assumed to be semi-rigidly connected. The buildings are subjected to three representative earthquakes. The evaluation of the results indicates that making the interior frames semi-rigid can lead to less story shear and lower column and connection moments and will increase the lateral load capacity of the building.

Key words: Semi-rigid steel frames, Welded connections, Bolted connections, Non-linear dynamic time history analysis, Seismic behavior, Connection rigidity.

Introduction

The 1994 Northridge Earthquake (USA) has shown the vulnerability of welded moment connections in steel moment resisting frames (MRFs) subject to severe earthquake ground motions (EQGMs). Since then, as an alternative connection type, bolted connections, often called semi-rigid connections, are considered for the retrofit and new design of steel MRFs in high seismicity regions. Steel frames with more flexible beam-to-column connections have also many economical and construction advantages over rigid frames. For collapse prevention under a severe EQGM, bolted semi-rigid frames are also an alternative. Typical bolted semi-rigid connections are dou-

ble web angles, single tee, top and bottom angles, top and bottom tees, extended end plate, top and bottom flange plates with web connections, and top and bottom angles with double web angles connections (Astaneh-Asl, 1994).

In seismic design, all steel frames are expected to suffer large inelastic deformation to dissipate energy during strong ground motion. In the current ASD (1989) and LRFD (1995) design codes, no analysis or design guidance is given for semi-rigid frames. In general, in the seismic design of steel buildings, the exterior frames of the building are assumed to be rigidly connected in one direction and the moment, due to both gravity and lateral loads, is transmitted by the connections to the columns, while the inte-

rior frames, in the same direction, are assumed to be pinned for resisting gravity loads and do not resist lateral forces. In the other direction, the frames are braced against earthquake or wind loads.

Moment resisting frames with rigid connections as well as braced frames with simple connections are defined in current seismic design codes and sufficient information is provided regarding the loading and resistance of these structural systems when subjected to earthquake loading (Sivakumaran, 1991). However, information on the seismic design and resistance of semi-rigid steel structures is scarce in the literature and current seismic code provisions do not provide the information necessary to design a semi-rigid steel frame, even though semi-rigid steel structures have been widely used for wind and gravity loads in modern steel structures (Akbas and Shen, 1995). There is only limited work in the literature about the rotational ductility and maximum plastic rotations required as well as the inter-story drift of semi-rigid connections subject to low or severe EQGM.

Nader and Astaneh-Asl (1991) have shown that semi-rigid connections do not experience a larger drift response than a rigid moment frame subject to different EQGMs. Akbas and Shen (1995) also studied steel frames with different height and connection parameters subject to various EQGMs. They showed that semi-rigid frames might experience larger drift response than rigid frames when subject to low or moderate intensity EQGMs. However, when subject to severe EQGMs, a larger drift response in semi-rigid frames than in rigid frames is not observed.

Some studies have also shown that semi-rigid steel frames have the potential to be used in buildings located in high seismic regions. A large number of semi-rigid steel structures have been designed and built in areas of moderate or low seismicity (Nader and Astaneh-Asl, 1992). More studies have been carried out experimentally with regard to the static behavior rather than the dynamic response of steel frames with semi-rigid connections before the 1990s (Harper *et al.*, 1990). Shen and Astaneh-Asl (1999) conducted a set of experimental studies to investigate the hysteretic behavior of bolted-angle connections. They concluded that bolted-angle connections have stable cyclic response and energy dissipation capacity depending on the size of the angles and bolts under cyclic loading and it is about four times the monotonic energy dissipation capacity. The stable cyclic behavior and energy dissipation capacity of

bolted semi-rigid frames may prevent the collapse of a hybrid system consisting of rigid frame and semi-rigid frames when the rigid frames experienced heavy damage after a severe EQGM. In another study by the same authors (Shen and Astaneh-Asl, 2000), a hysteresis model for bolted angles is proposed for seismic analyses.

This paper investigates the seismic design and performance of a hybrid system consisting of welded moment frames and bolted semi-rigid frames. Welded moment frames have higher initial stiffness and bolted semi-rigid frames have better post-yielding performance. The objective of the present study is to evaluate and compare the seismic response of both rigid steel moment resisting frames and hybrid systems. For this purpose, nonlinear dynamic time history analyses on two steel buildings having rigid and semi-rigid steel frames with different connections are carried out. The analytical study is highlighted as follows:

1. designing two steel buildings, of 5 and 10 stories based on seismic code provisions,
2. carrying out nonlinear dynamic time history analyses on rigid frames,
3. introducing connection flexibility on interior frames and carrying out nonlinear dynamic time history analyses on the hybrid system, and
4. evaluating and comparing the results obtained from steps 2 and 3.

Connection Parameters for a Semi-Rigid Connection

Steel frames are divided into three types: rigid or fully restrained (*FR*), semi-rigid or partially restrained (*PR*), and simple (LRFD, 1995). Rigid connections are capable of developing a moment at the beam end more than or equal to 90% of the fixed end moment, while pinned connections can only develop a moment at the beam end less than 20% of the fixed end beam (Astaneh-Asl, 1989; Nader and Astaneh-Asl, 1992). By using the well-known beam line equation, from the above definition it is concluded that a connection is to be considered rigid if its rotational stiffness is at least $(18EI/L)_b$ and to be pinned if it is less than or equal to $(EI/2L)_b$. A semi-rigid connection's rotational stiffness lies between $(EI/2L)_b$ and $(18EI/L)_b$, i.e. a semi-rigid connection can be

defined as one that is more flexible than a rigid connection, but stiffer than a pinned one (Nader and Astaneh-Asl, 1992).

The following two parameters can be used to define the stiffness and strength of a semi-rigid connection.

Relative rotational stiffness (β)

The relative rotational stiffness (β) of a semi-rigid connection is defined as the ratio of the elastic rotational stiffness of the connection to the elastic bending stiffness of the connected beam.

$$\beta = (K_e)_{con}/(EI/L)_{beam} \quad (1)$$

where $(K_e)_{con}$ is the elastic rotational stiffness of the connection, and $(EI/L)_{beam}$ is the elastic bending stiffness of the connected beam. In Eq. (1), the beam is assumed to remain elastic. It should be noted that in the seismic design of steel MRFs, the general design philosophy is to make the connection stronger and stiffer than the beam and to make sure that the connection behaves elastically during a severe EQGM. However, in the seismic design of semi-rigid frames, beams behave elastically and the semi-rigid connections are designed to have less bending capacity and stiffness and to behave inelastically during a severe EQGM (Astaneh, 1994). A steel connection is said to be rigid if β is equal to or greater than 18, to be pinned if β is less than 0.5, and to be semi-rigid if β is between 0.5 and 18 (Nader and Astaneh-Asl, 1992).

Relative Strength Ratio (α)

The relative strength ratio (α) of a connection is defined as the ratio of the plastic moment capacity of the connection to the plastic moment capacity of the connected beam.

$$\alpha = (M_p)_{con}/(M_p)_{beam} \quad (2)$$

where $(M_p)_{con}$ is the plastic moment capacity of the connection, and $(M_p)_{beam}$ is the plastic moment capacity of the beam. Based on experimental studies, Nader and Astaneh-Asl (1992) recommended that α lie between 0.70 and 1.00 for top and bottom flange plate connections, 0.65 and 1.00 for extended end plate connections, and 0.50 and 0.75 for top and bottom angle connections.

Seismic Design of Frames

To evaluate and compare the dynamic response of steel frames with combined rigid and semi-rigid frames, two buildings, of 5 and 10 stories, with different beam-to-column semi-rigid connections are investigated. The planes of the buildings are symmetrical and have two rigid perimeter frames in both directions (Figure 1). Both buildings consist of four-bay frames spaced at 915 cm and the story height is 366 cm, except at the first level where it is 427 cm (Figure 2). Two sets of design analyses are performed on the buildings. In the first set of analyses, the two exterior frames are assumed to be rigidly connected, while the three interior frames are simply supported and make no contribution to carrying lateral loads (Case 1). Member sizes obtained from the first set of analyses are given in Figure 2 for the 5- and 10-story buildings. In the second set of analysis, the two exterior frames are again assumed to be rigidly connected, while semi-rigidity is introduced into the three interior frames, which will contribute to carrying lateral loads (Case 2). Member sizes obtained from the second set of analyses are given in Figures 3 and 4 for 5- and 10-story buildings, respectively.

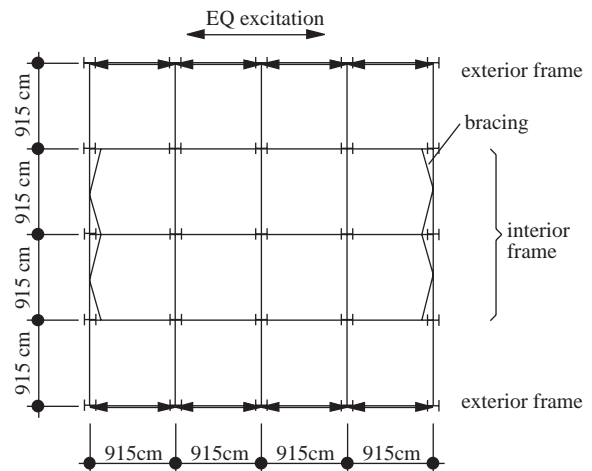


Figure 1. Typical floor framing plan.

A dead load of 4.80 kN/m² and live load of 2.40 kN/m² are used in the load combinations of $1.4(\text{dead load}) + 1.6(\text{live load})$ and $1.2(\text{dead load}) + 0.5(\text{live load}) + 1.5(\text{earthquake})$ for all members, except the roof floor, at which a dead load of 3.85 kN/m² and live load of 1.00 kN/m² are used in the load combinations. LRFD (1995) code provisions are used in the design. All of the beams and columns are specified

as A36 ($F_y = 250$ Mpa) steel. Strong column-weak beam requirement is satisfied in the design of rigid frames. The design base shears of the frames are determined by UBC-94 (1994). Both buildings are assumed to be built on stiff soil and located in seismic zone 1. The seismic masses of the structures are 3134 t ($\text{kN}\cdot\text{s}^2/\text{m}$) and 6399 t ($\text{kN}\cdot\text{s}^2/\text{m}$) for the 5- and 10-story buildings, respectively. The total base shears are 1526 kN and 2046 kN for 5- and 10-story buildings, respectively.

Seismic Analysis of the Frames

The floor system of the buildings is assumed to provide diaphragm action and to be rigid in the horizontal plane. The two-dimensional models of the frames are built for nonlinear dynamic time history analysis using a general-purpose nonlinear dynamic analysis program, DRAIN-2DX (Prakash *et al.*, 1994). For the nonlinear dynamic analyses of the hybrid system, rigid frames and semi-rigid frames are modeled two-dimensionally using infinitely rigid links at story

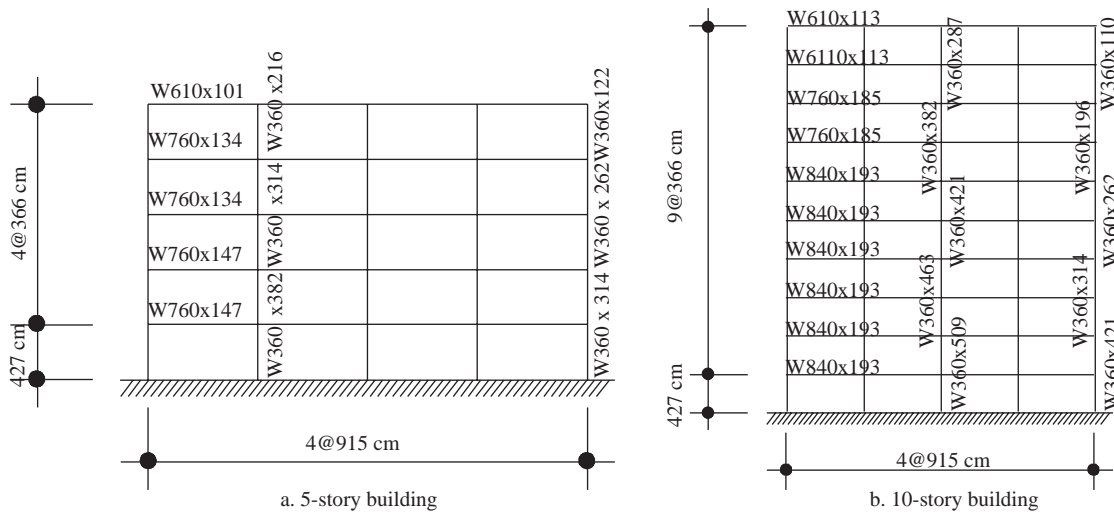


Figure 2. Elevation and member sizes of the exterior frames of the 5- and 10-story buildings (Case 1 – interior frames are simply supported).

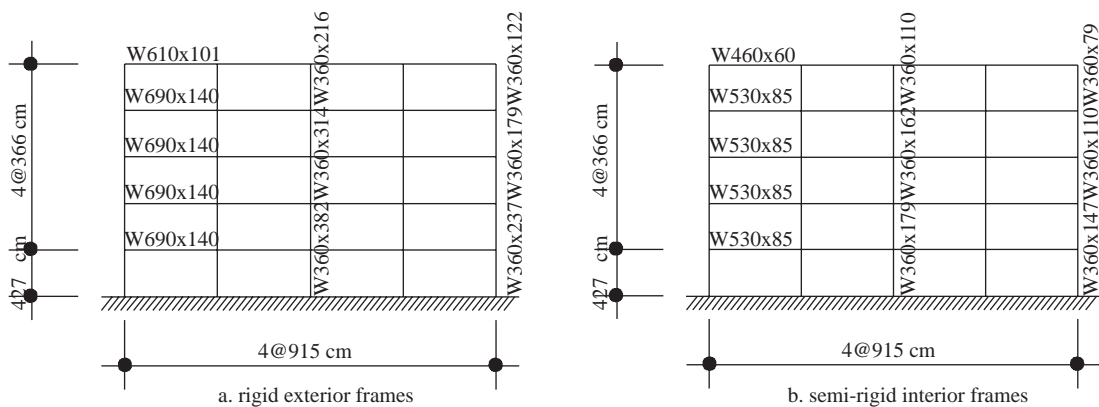


Figure 3. Elevation and member sizes of the 5-story building (Case 2).

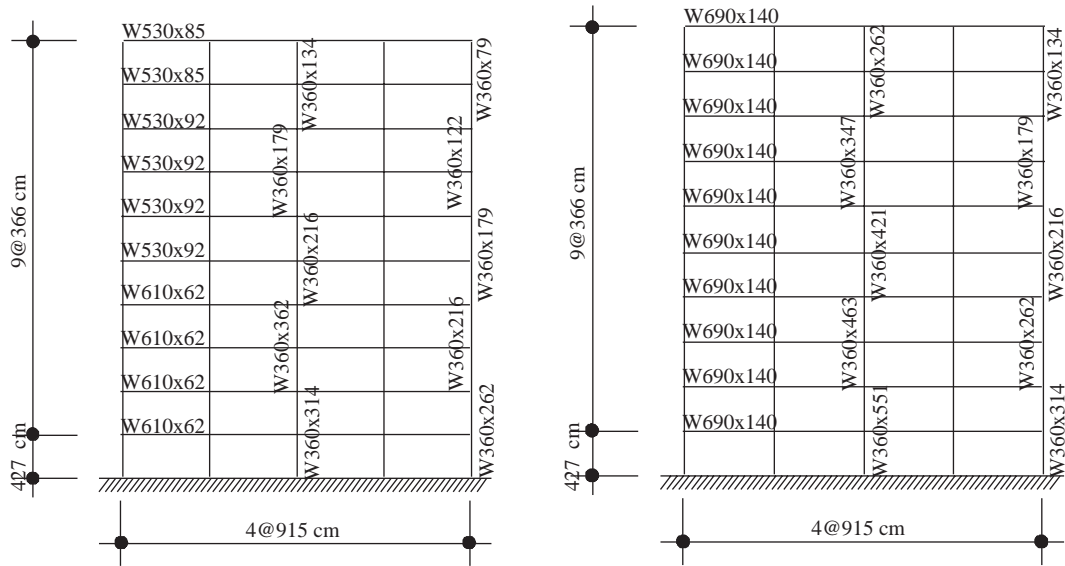


Figure 4. Elevation and member sizes of the 10-story building (Case 2).

levels. The inertial effects of each story level are assumed to be carried by each perimeter MRF and they resist one half of the seismic mass of the entire building for Case 1. For Case 2, the inertial effects of each story level are assumed to be carried by each perimeter MRF and three interior semi-rigid frames and each frame resists only the portion of the seismic mass of the entire building obtained from the tributary area of each frame. Beam-column elements are used in the analysis. Inelastic effects are assigned to plastic hinges at member ends. Strain hardening is taken to be 5% in all elements. Semi-rigid connection elements for different α and β values are arranged at each beam-to-column connection for the semi-rigid frames in the second set of analysis (Case 2). P-M (axial load-moment) interaction relation, suggested by LRFD (1995), is used as a yielding surface of column elements. Beams and columns have a bilinear moment-rotation relationship. Rotational connection elements are specified to behave inelastically. P- Δ effect is not considered in the analysis.

The buildings are subjected to three representative EQGMs, El Centro, Northridge and Olympia. The characteristics of these EQGMs are given in Table 1. Strong motion duration (t_D) and predominant ground motion period (T_g) are also included in Table 1. Different types of soil conditions, strong motion durations, distances and magnitudes can be treated in the analyses using these ground motions to obtain the most serious response from the buildings. The selected EQGMs have different peak ground accelera-

tions and strong motion durations (t_D) ranging from 5.50 s to 24.46 s (Table 1). Nonlinear dynamic time history analyses are performed for both buildings by scaling the maximum ground acceleration ($\ddot{u}_{g,max}$) of the three earthquakes to 0.3g, corresponding to a moderate level of EQGM, and 0.6g, corresponding to a severe EQGM, where g is acceleration due to gravity. Mass is assumed to be lumped at the joints. The damping ratio is assumed to be 2% and Rayleigh damping with first and third natural frequency and with first and sixth natural frequency for the 5- and 10-story buildings, respectively, is used in the analyses.

The buildings are analyzed for 15 different combinations of varying β (0.001, 1, 4, 8, 12) and α (0.2, 0.5, 0.75) values for each of the selected earthquakes and each case (Cases 1 and 2). $\beta = 0.001$ corresponds to a pin connection in which case the semi-rigid interior frames do not contribute in carrying seismic forces.

Results

The nonlinear seismic response of buildings with combined rigid and semi-rigid frames are evaluated and compared in terms of the variation of fundamental natural period versus relative rotational stiffness, roof displacement envelopes story shear envelopes, drift ratio envelopes, and energy input. Pushover analyses are also carried out on the buildings and compared for different combinations of α and β . Comparison of the results obtained from the non-

linear dynamic time history analyses of the buildings (Figures 5 through 13) reveals that the effect of semi-rigidity on traditional steel building construction is considerable. Due to space limitations, the results are presented only for El Centro EQGM and $\ddot{u}_{g,\max} = 0.6g$. Detailed results can be found in Akbas and Shen (2003).

Variation of fundamental natural period

Variation of fundamental natural period with respect to α shows that there is a significant period change for both 5- and 10-story buildings as α increases and semi-rigid interior frames start being almost rigidly connected ($\alpha = 25$) and contribute significantly to carrying seismic forces. Decrease in period from $\alpha = 0$ to $\alpha = 25$ is 54.4% (from 1.25 s to 0.57 s) and 46.3% (from 2.03 s to 1.09 s) for 5- and 10-story buildings, respectively (Akbas and Shen, 2003). It is clear that as α increases and semi-rigid interior frames start contributing to the carrying of lateral loads, the buildings become more rigid and attract more shear force.

Roof displacement envelopes

Roof displacement envelopes of the 5-story building are given in Figure 5 for El Centro EQGM, $\ddot{u}_{g,\max} = 0.6g$, and $\beta = 4$ and 12. The “rigid frames”

line in all the figures (Figures 5 through 13) refers to Case 1. All of the other lines in all the figures for different values of α (Figures 5 through 13) refer to Case 2. As can be observed from Figure 5, in general, Case 2 experiences less displacement than Case 1 for any value of α . This is an expected result due to the decreasing period of the buildings. The effect of α on roof displacement is much more apparent with increasing values of β . Case 2 tends to experience less displacement as β increases.

Roof displacement envelopes for the 10-story building are given in Figure 6 for El Centro EQGM, $\ddot{u}_{g,\max} = 0.6g$, and $\beta = 4$ and 12. The same observations can be made for the 10-story building as for the 5-story building. Case 2 experiences less displacement than Case 1 for any value of α and Case 2 tends to experience less displacement as β increases.

Story shear envelopes

Story shear envelopes for the 5-story building are given in Figure 7 for El Centro EQGM, $\ddot{u}_{g,\max} = 0.6g$, and $\beta = 4$ and 12. Case 1, in general, experiences less shear than Case 2 as α and β increases. Case 2 tends to experience more shear force as β increases and α has no effect on story shear force for very small values of β (>1) (Akbas and Shen, 2003), while the effect of α on story shear is much more apparent with increasing values of β (Figure 7).

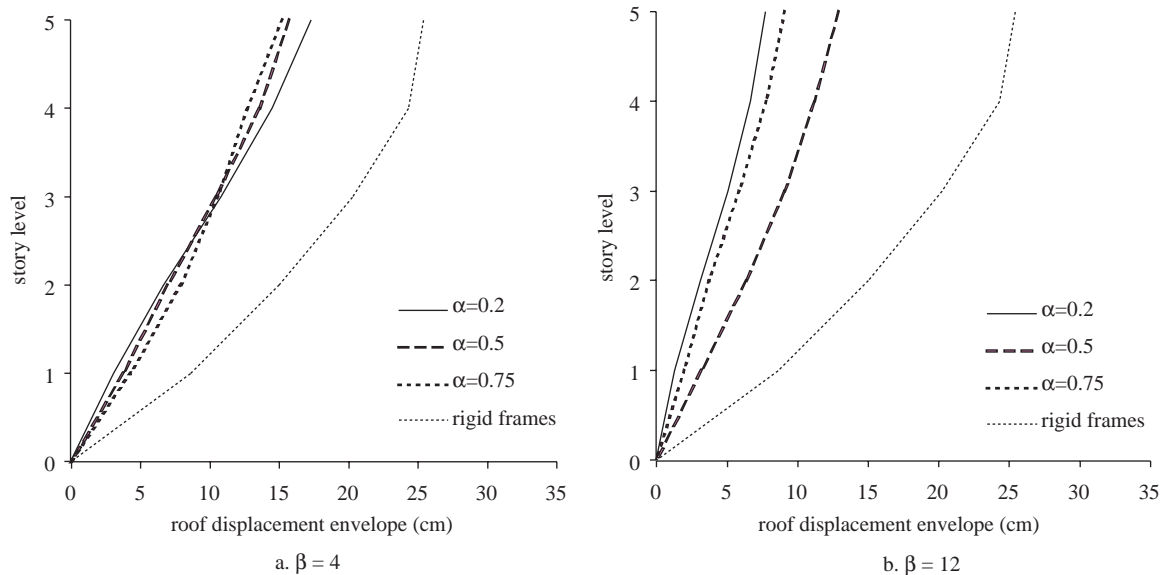


Figure 5. Roof displacement envelopes of the 5-story building for El Centro EQGM, $\ddot{u}_{g,\max} = 0.6g$.

Table 1. Earthquake ground motion characteristics.

Earthquake	Comp.	M_L	Focal Depth	Epicentral Distance (g)	$\ddot{u}_{g,max}$ (cm)	$\dot{u}_{g,max}$ (s)	T_g (s)	t_D	Geology
El Centro May 18, 1940	S00E	6.3	16	9.3	0.3489	33.45	0.43	24.46	30 m stiff clay, volcanic rock
Northridge Jan. 17, 1994	NEW-360	6.4	19	19.2	0.5963	56.90	0.68	5.50	organic clays up to 6.1 m below ground surface
Olympia April 13, 1949	N04W	7.1	N/A	39	0.1661	21.41	0.23	21.64	N/A

M_L = earthquake magnitude; $\ddot{u}_{g,max}$ = peak ground acceleration; $\dot{u}_{g,max}$ = peak ground velocity; T_g = predominant ground motion period; t_D = strong motion duration

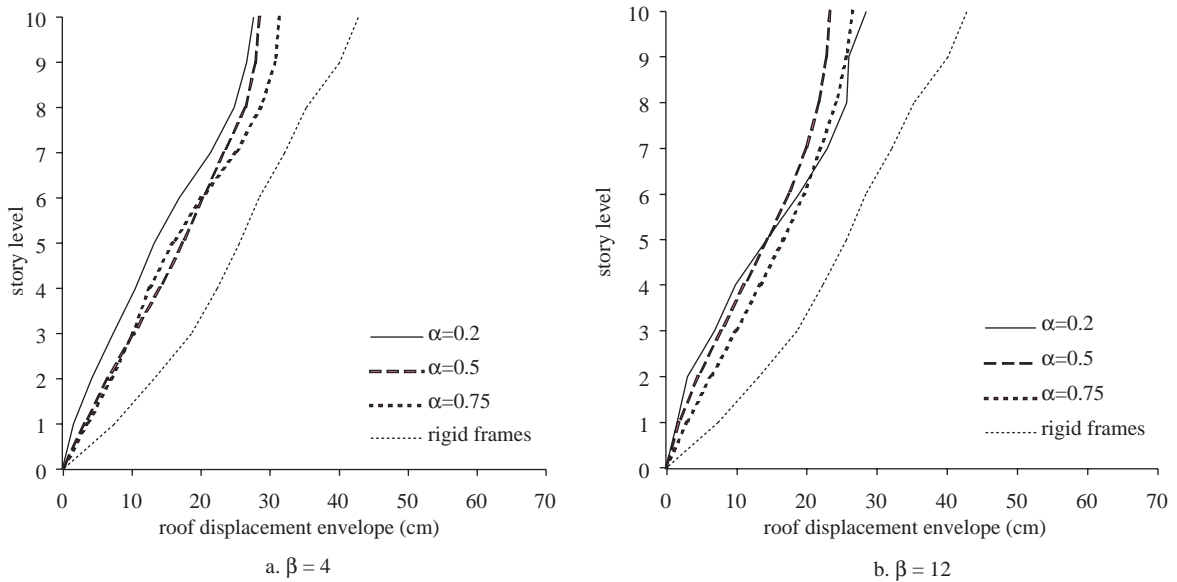


Figure 6. Roof displacement envelopes of the 10-story building for El Centro EQGM, $\ddot{u}_{g,max} = 0.6g$.

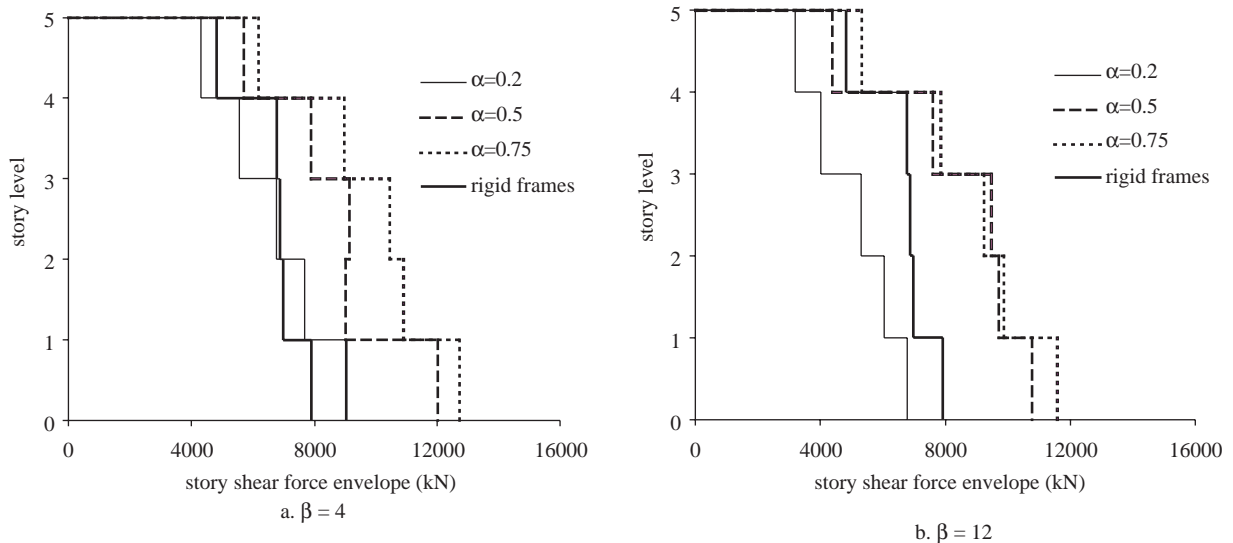


Figure 7. Story shear force envelopes of the 5-story building for El Centro EQGM, $\ddot{u}_{g,max} = 0.6g$.

Story shear envelopes for the 10-story building are given in Figure 8 for El Centro EQGM, $\ddot{u}_{g,max} = 0.6g$, and $\beta = 4$ and 12. Case 2 experiences, in general, less shear than Case 1 as α and β increases for $\ddot{u}_{g,max} = 0.3g$ (Akbas and Shen, 2003), while Case 1 experiences, in general, less shear than Case 2 as α and β increases for $\ddot{u}_{g,max} = 0.6g$ (Figure 8). Case 2 tends to experience more shear as β increases and α has no effect on story shear for very small values of β (>1) (Akbas and Shen, 2003), while the effect of α on story shear is much more apparent with increasing values of β (Figure 8).

Drift ratio envelopes

Drift ratio envelopes for the 5-story building are given in Figure 9 for El Centro EQGM, $\ddot{u}_{g,max} = 0.6g$, and $\beta = 4$ and 12. Case 2 experiences less drift than Case 1 as α and β increases and Case 2 tends to experience less drift as β increases. α has no effect on drift ratio for very small values of β (>1) (Akbas and Shen, 2003), while the effect of α on drift ratio is much more apparent with increasing values of β (Figure 9).

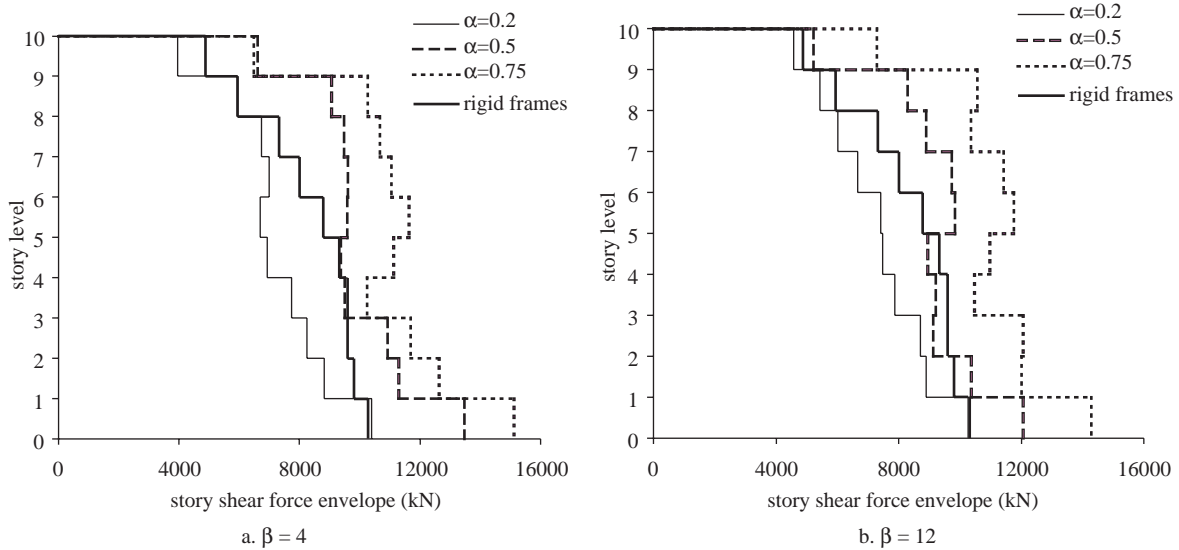


Figure 8. Story shear force envelopes of the 10-story building for El Centro EQGM, $\ddot{u}_{g,max} = 0.6g$.

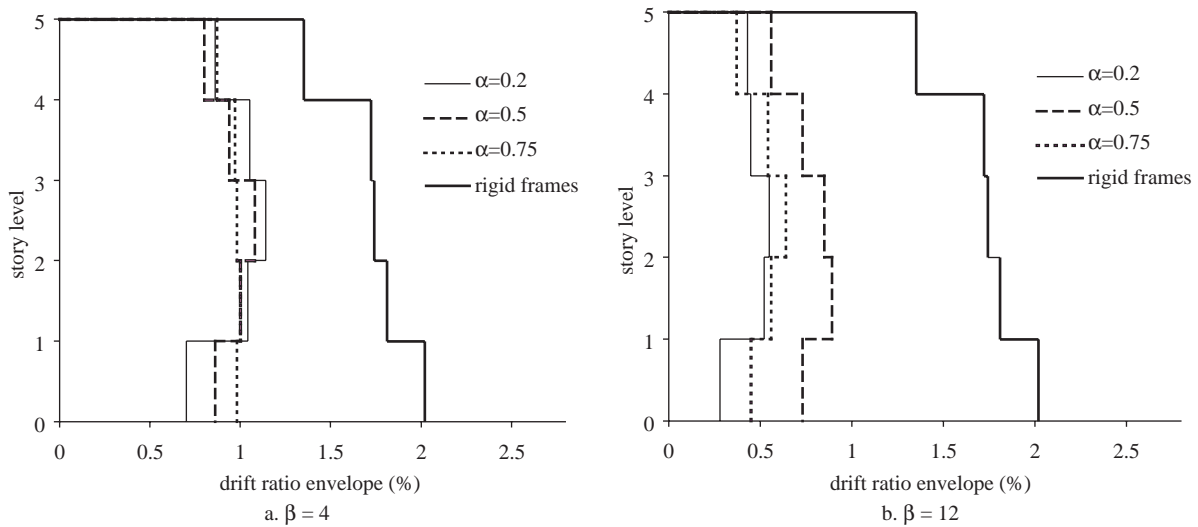


Figure 9. Drift ratio envelopes of the 5-story building for El Centro EQGM, $\ddot{u}_{g,max} = 0.6g$.

Drift ratio envelopes for the 10-story building are given in Figure 10 for El Centro EQGM, $\ddot{u}_{g,max} = 0.6g$, and $\beta = 4$ and 12. Similar observations can be made for the 10-story building as for the 5-story building. Case 2 experiences less drift than Case 1 as α and β increases and Case 2 tends to experience less drift as β increases. α has no effect on drift ratio for very small values of β (>1) (Akbas and Shen, 2003), while the effect of α on drift ratio is much more apparent with increasing values of β (Figure 10).

Energy input

Energy input values for the 5-story building are given in Figure 11 for El Centro EQGM, $\ddot{u}_{g,max} = 0.6g$, and $\beta = 4$ and 12. The lower part of the bars in the figures, shown with longitudinal thin solid lines, shows the amount of hysteretic energy, while the upper part, shown with a horizontal thin solid line, shows the amount of damping energy. Energy input is the sum of both hysteretic and damping energies. α has no significant effect on energy input for very small values of β (>1) (Akbas and Shen, 2003), while the effect of α on energy input is much more apparent with increasing values of β (Figure 11).

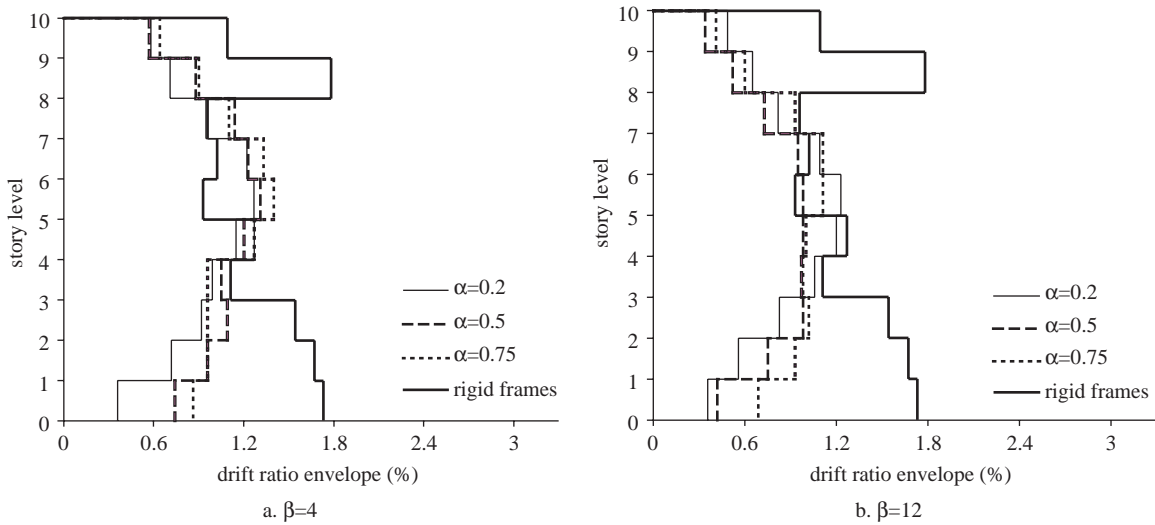


Figure 10. Drift ratio envelopes of the 10-story building for El Centro EQGM, $\ddot{u}_{g,max} = 0.6g$.

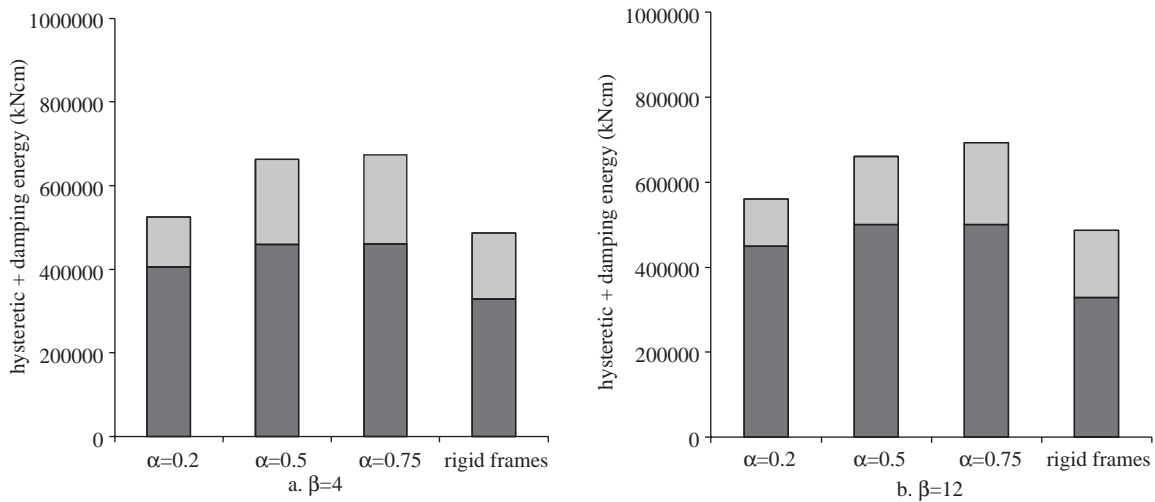


Figure 11. Energy input of the 5-story building for El Centro EQGM, $\ddot{u}_{g,max} = 0.6g$.

Energy input values for the 10-story building are given in Figure 12 for El Centro EQGM, $\ddot{u}_{g,max} = 0.6g$, and $\beta = 4$ and 12. The same observations can be made for the 10-story frame as for the 5-story frame. α has no significant effect on energy input for very small values of β (>1) (Akbas and Shen, 2003), while the effect of α on energy input ratio is much more apparent with increasing values of β (Figure 12).

Pushover analysis

Pushover static analyses are performed for triangular load distribution for both buildings. The lat-

eral force is increased until the roof displacement reached 250 cm for all frames. Results from the static pushover analyses are given in the form of V/W versus roof displacement, where V is total base shear and W is total weight of the building. Pushover analyses results for the 5-story building are given in Figure 13a. β has no effect on the V/W ratio for $\alpha = 0.001$ (Akbas and Shen, 2003), while the effect of β is much more apparent with increasing values of α (Figure 13a). Case 2 is, in general, more rigid than Case 1 in both elastic and inelastic regions (Figure 13a).

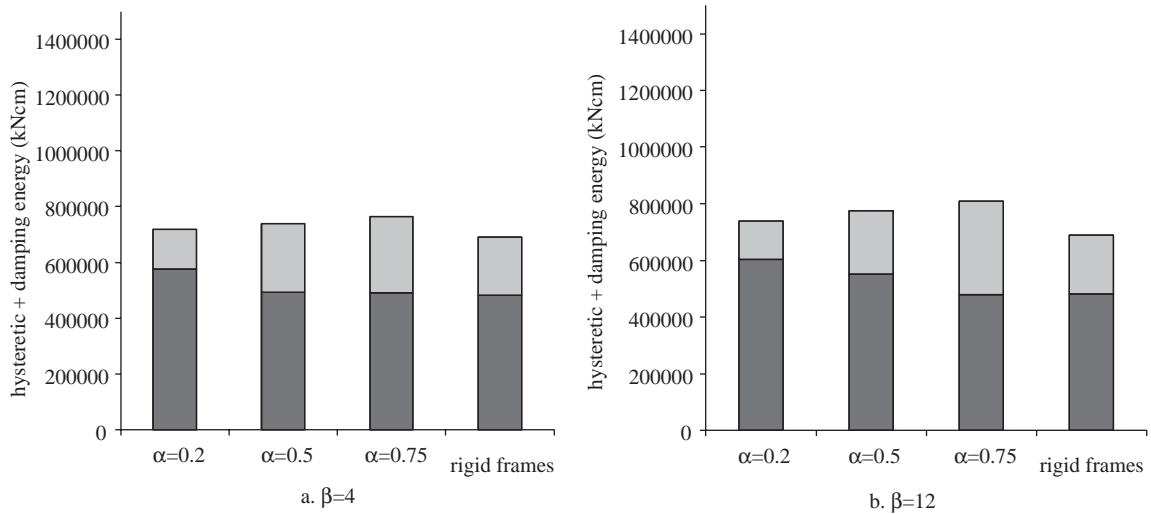


Figure 12. Energy input of the 10-story building for El Centro EQGM, $\ddot{u}_{g,max} = 0.6g$.

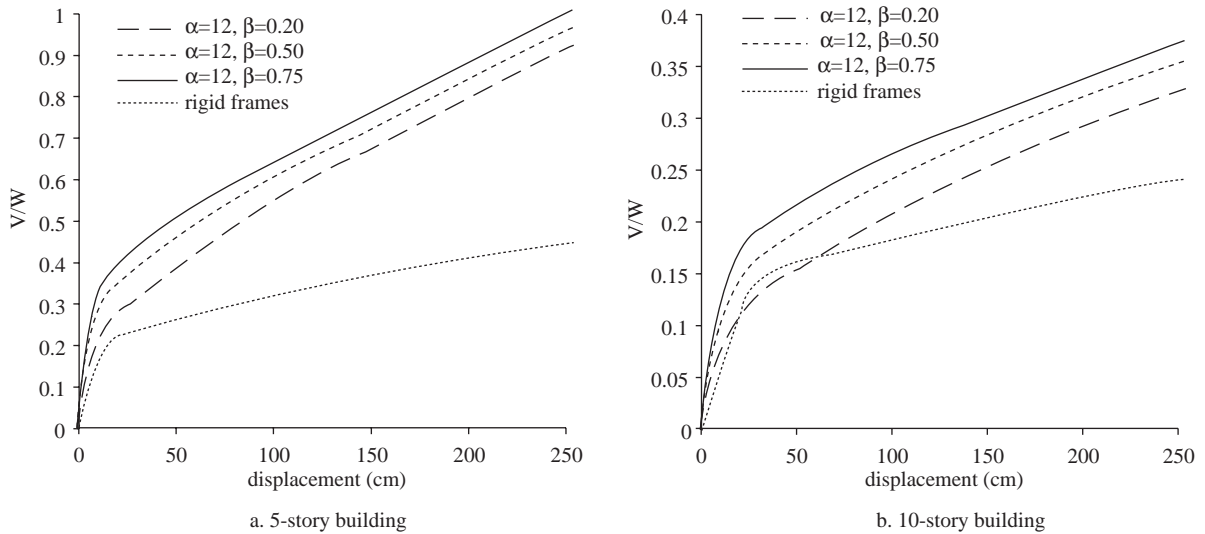


Figure 13. Pushover analysis.

Results of pushover analyses for the 10-story building are given in Figure 13b. Similar observations can be made for 10-story building as for the 5-story building. β has no effect for $\alpha = 0.001$ (Akbas and Shen, 2003), while the effect of β is much more apparent with increasing values of α (Figure 13b). Case 2 is, in general, more rigid than Case 1 in both the elastic and inelastic regions (Figure 13b).

Conclusions

From the analyses of the results obtained in this study, the following conclusions can be made:

1. Steel buildings with combined rigid and semi-rigid frames might have high performance under a moderate intensity EQGM and the stiffness of this hybrid system is mainly contributed by the rigid frames. However, when subject to a severe EQGM, semi-rigid frames resist a significant portion of the seismic force in this hybrid system and this causes less stress concentration in the rigid frames.
2. This study shows that bolted semi-rigid steel frames might be used with rigid steel MRFs in high seismicity regions. However, it should be kept in mind that this is an analytical investigation based on simple assumptions.
3. The connection parameters α and β used in this study significantly affect the overall seismic response of the hybrid system.

4. Steel buildings with combined rigid and semi-rigid frames might reduce the seismic force in rigid frames.
5. Relative stiffness (β) and relative strength ratio (α) are two key parameters in evaluating the dynamic response of a hybrid system.

Nomenclature

F_y	yield strength [Mpa]
$(EI/L)_{beam}$	elastic bending stiffness of the connected beam
$(K_e)_{con}$	elastic rotational stiffness of the connection
M	moment [Nmm]
$(M_p)_{con}$	plastic moment capacity of the connection [Nmm]
$(M_p)_{beam}$	plastic moment capacity of the beam [Nmm]
P	axial load [N]
T_g	predominant ground motion period [s]
V	total base shear [N]
W	total weight of the building [N]
g	acceleration due to gravity [mm/s^2]
t_D	strong motion duration [s]
α	relative rotational stiffness
β	relative strength ratio
Δ	lateral displacement [mm]
$\ddot{u}_{g,max}$	peak ground acceleration [mm/s^2]

References

- AISC-ASD, Allowable Stress Design, American Institute of Steel Construction, Chicago, 1989.
- AISC-LRFD, "Load and Resistance Factor Design, American Institute of Steel Construction, Chicago, 1995.
- Akbas, B. and Shen, J. "Seismic Design Study of P- Δ Effect On Steel Frames with Various Connections", Proceedings of Seventh Canadian Conference on Earthquake Engineering, Montreal, Canada, 525-532, June 5-7, 1995.
- Akbas, B. and Shen, J. "Effect of Interior Semi-Rigid Frames on the Seismic Behavior of Steel Moment Resisting Frames", Report No. GYTE-EQ&S-03/001, Department of Earthquake and Structural Science, Gebze Institute of Technology, 2003.
- Astaneh-Asl, A. "Demand of Supply of Ductility in Steel Shear Connections", Journal of Constructural Steel Research, 14, 1-19, 1989.
- Astaneh-Asl, A. "Seismic Behavior and Design of Steel Semi-Rigid Structures", Proceedings of the STESSA '94, Behavior of Steel Structures in Seismic Areas, ed. by F.M. Mazzolani and V. Gioncu, 1994.
- Harper, W.L., Dickerson, J.R., Bradburn, J.H. and Radziminski, J.B. "Static of Cyclic Behavior of Semi-Rigid Bolted of Welded Beam-Column Connections", Structural Steel Research Studies, University of South Carolina, Columbia, South Carolina, 1990.
- Nader, M.N. and Astaneh-Asl, A., "Dynamic Behavior of Flexible, Semi-Rigid and Rigid Steel Frames", Journal of Constructional Steel Research, 18, 179-192, 1991.
- Nader, M.N. and Astaneh-Asl, A., "Seismic Behavior and Design of Semi-Rigid Steel Frames", Earthquake Engineering Research Center, Report

No. UCB/EERC-92/06, University of California at Berkeley, 1992.

Prakash, V., Powell, G.H., and Campbell, S. "DRAIN-2DX User Guide V.1.10", Department of Civil Engineering, University of California at Berkeley, 1993.

Sivakumaran, K.S. "Seismic Response of Unbraced Steel Frames", Earthquake Engineering and Structural Dynamics, 20, 1029-1043, 1991.

Shen, J. and Astaneh-Asl, A., "Hysteretic Behavior of Bolted-Angle Connections", Journal of Constructional Steel Research, 51, 201-218, 1999.

Shen, J. and Astaneh-Asl, A., "Hysteretic Model of Bolted-Angle Connections", Journal of Constructional Steel Research, 54, 317-343, 2000.

UBC-94, Uniform Building Code, International Conference of Building Officials, 1994.